Quantum Chemical Conformational Analysis of Glucose in Aqueous Solution

Christopher J. Cramer* and Donald G. Truhlar*

Contribution from the Department of Chemistry and Supercomputer Institute, University of Minnesota, Minneapolis, Minnesota 55455-0431

Received January 20, 1993

Abstract: We have calculated the aqueous solvation effects on the anomeric and conformational equilibria of D-glucopyranose using a quantum chemical solvation model based on a continuum treatment of dielectric polarization and solvent accessible surface area. The solvation model puts the relative ordering of the hydroxymethyl conformers in line with the experimentally determined ordering of populations. Our calculations indicate that the anomeric equilibrium is controlled primarily by effects that are also present in the gas-phase potential energy function, that the *gauche*/*trans* O–C(6)–C(5)–O hydroxymethyl conformational equilibrium is dominated by favorable solute–solvent hydrogen bonding interactions, and that other rotameric equilibria are controlled mainly by dielectric polarization of the solvent. The description of the aqueous free energy changes of the latter require at least a distributed monopole representation since they do not correlate with overall dipole moment. We also find evidence for intra-glucose hydrogen bond conjugation in aqueous solution.

1. Introduction

Conformational behavior of simple sugars plays a critical role in determining the structure of more complicated molecules in which they function as subunits, e.g., polysaccharides,[1-3] cyclodextrins,[4] and glycoproteins.[5] Especially challenging to modeling efforts is understanding the factors that influence aqueous conformational stability of sugars with respect to biomolecular function, e.g., inhibitor binding, allosteric regulation, and molecular recognition.[1,6,7]

Even a monosaccharide like glucose, which exists almost entirely in the pyranose form in aqueous solution, poses a tremendous challenge to molecular theory because of the many torsional degrees of freedom present in the pyranose. Rotation about the C–O bonds of the hydroxyl groups, as well as the C(5)–C(6) bond, potentially affords three distinct energy minima for the various staggered arrangements about each rotating bond. Additionally, one must consider both the α and β anomers of the sugar, and finally there are two distinct chair forms of the pyranose related by a ring flip. This gives rise to $2 \times 2 \times 3^6 = 2916$ potential conformers which should be sampled in a thorough exploration of the hypersurface! Of course, some of the conformations may be ruled out by simple stereochemical considerations. In glucose, for instance, one of the two pyranose chairs would place all non-anomeric substituents axial and may thus be ignored as energetically unreasonable. Nevertheless, exploring the conformational energy hypersurface remains daunting.

Glucose has been the subject of recent theoretical studies.[8-11] The focus has primarily been on explaining the anomeric equilibrium, in which, experimentally,[12] the β-D [equatorial C(1)–OH] anomer is more stable than the α-D [axial C(1)–OH] anomer by about 0.3 kcal/mol in aqueous solution. Additionally, various conformations associated with internal rotation of the C(5)–C(6) and C(6)–O bonds have been explored. The $\bar{G}$, G, and T conformations associated with the C(5)–C(6) internal rotation are illustrated in Figure 1, where the letter refers to the O–C(6)–C(5)–O dihedral angle (either *gauche* or *trans*), and the $\bar{G}$ and G notations distinguish the two possible associated O–C(6)–C(5)–C(4) dihedrals. In particular, the G conformer has a *trans* O–C(6)–C(5)–C(4) dihedral, and the $\bar{G}$ has this dihedral *gauche*. Experimental observation suggests that the $\bar{G}$ and G conformations are populated in about a 55:45 ratio at room temperature, while the T is populated no more than about 2%.[13] (Experiments on 2-acetamido-2-deoxy-D-glucose have been interpreted as indicating 75% $\bar{G}$ and 25% T,[14] but as discussed elsewhere,[3] the interpretation of ref 13 agrees better with crystal data and is more widely accepted.) Solute–solvent hydrogen bonding and additional solute conformations resulting from rotation of the remaining hydroxyl groups have also received attention in the theoretical studies.[8-11]

The anomeric effect[1,12,15-19] in pyranose rings is the tendency for electron-withdrawing groups at C(1) to increase the population of the axial (α-D) orientation at the expense of the sterically

* Correspondence may be addressed to either author.

(1) Lemieux, R. U. *Explorations with Sugars: How Sweet it Was*; American Chemical Society: Washington, DC, 1990.

(2) (a) Cumming, D. A.; Carver, J. P. *Biochemistry* **1987**, *26*, 6664, 6676. (b) Rademacher, T. W.; Parekh, R. B.; Dwek, R. A. *Annu. Rev. Biochem.* **1988**, *57*, 785. (c) Edge, C. J.; Singh, U. C.; Bezzo, R.; Taylor, G. L.; Rademacher, T. W. *Biochemistry* **1990**, *29*, 1971. (d) Carver, J. P. *Current Opinion Struct. Biol.* **1991**, *1*, 716. (e) Penhoat, C. H. d.; Imberty, A.; Roques, N.; Michon, V.; Mentech, J.; Descotes, G.; Pérez, S. *J. Am. Chem. Soc.* **1991**, *113*, 3720. (f) Dowd, M. K.; French, A. D.; Reilly, P. J. *Carbohydr. Res.* **1992**, *233*, 15. (g) Zhbankov, R. G. *J. Mol. Struct.* **1992**, *275*, 65.

(3) Kroon-Batenburg, L. M. J.; Kroon, J. *Biopolymers* **1990**, *29*, 1243.

(4) Koehler, J. E. H.; Saenger, W.; Van Gunsteren, W. F. *J. Mol. Biol.* **1988**, *203*, 241.

(5) (a) Paulsen, H. *Angew. Chem., Int. Ed. Engl.* **1990**, *29*, 823. (b) *Chem. Eng. News*, **1992**, March 23, 37.

(6) (a) Srivastava, O. M.; Hindsgaul, O.; Shoreibah, M.; Pierce, M. *Carbohydr. Res.* **1988**, *179*, 137. (b) Ragazzi, M.; Ferro, D. R.; Perly, B.; Petitou, M.; Choay, J. *Carbohydr. Res.* **1990**, *195*, 169. (c) Sabesan, S.; Bock, K.; Paulson, J. C. *Carbohydr. Res.* **1991**, *218*, 27.

(7) (a) Avery, O. T.; Heidelberg, M. *J. Exp. Med.* **1923**, *38*, 81. (b) Aminoff, D.; Morgan, W. T. J. *Nature* **1948**, *162*, 579. (c) Hakomori, S.; Nudelman, E.; Kannagi, R.; Levery, S. B. *Biochem. Biophys. Res. Commun.* **1982**, *109*, 36. (d) Israel, M.; Murray, R. J. *J. Med. Chem.* **1982**, *25*, 24. (e) Lemieux, R. U. et al. *Can. J. Chem.* **1985**, *63*, 2664. (f) Walker, S.; Valentine, K. G.; Kahne, D. *J. Am. Chem. Soc.* **1990**, *112*, 6428. (g) Lee, M. D.; Ellestad, G. A.; Borders, D. B. *Acc. Chem. Res.* **1991**, *24*, 235. (h) Rao, V. S. R. In *Molecular Conformation and Biological Interactions*; Balaram, P., Ramaseshan, S., Eds.; Indian Academy of Sciences: Bangalore, 1991; p 411. (i) Nicolaou, K. C.; Dai, W.-M.; Tsay, S.-C.; Estevez, V. A.; Wrasidlo, W. *Science* **1992**, *256*, 1172.

(8) Brady, J. W. *J. Am. Chem. Soc.* **1989**, *111*, 5155.

(9) Van Eijck, B. P.; Kroon-Batenburg, L. M. J.; Kroon, J. *J. Mol. Struct.* **1990**, *237*, 315.

(10) Ha, S.; Gao, J.; Tidor, B.; Brady, J. W.; Karplus, M. *J. Am. Chem. Soc.* **1991**, *113*, 1553.

(11) Polavarapu, P. L.; Ewig, C. S. *J. Comput. Chem.* **1992**, *13*, 1255.

(12) (a) Angyal, S. J. *Aust. J. Chem.* **1968**, *21*, 2737. (b) Angyal, S. J. *Angew. Chem., Int. Ed. Engl.* **1969**, *8*, 157.

(13) Nishida, Y.; Ohrui, H.; Meguro, H. *Tetrahedron Lett.* **1984**, *25*, 1575.

(14) Boyd, J.; Porteous, R.; Suffe, N.; Delepierre, M. *Carbohydr. Res.* **1985**, *139*, 35.

(15) Edward, J. T. *Chem. Ind. (London)* **1955**, 1102.

(16) Tvaroška, I.; Bleha, T. *Adv. Carbohydr. Chem. Biochem.* **1989**, *47*, 45.

0002-7863/93/1515-5745$04.00/0

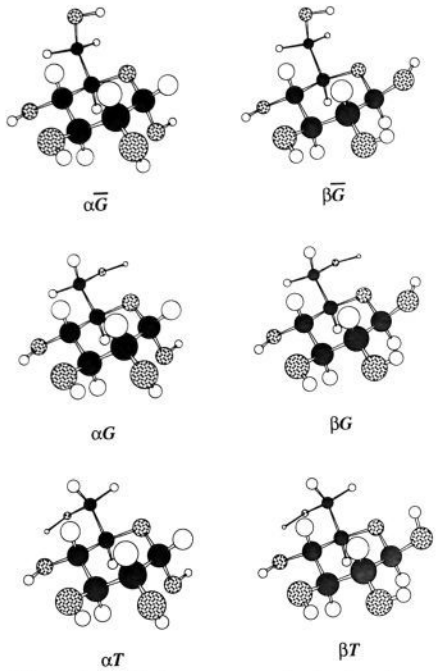

Figure 1. Illustration of the lowest-energy ring hydroxyl rotamers for the $\bar{G}$, G, and T hydroxymethyl conformers of both anomers of D-glucose calculated at the AM1 level.

favored equatorial (β-D) orientation. Considerable theoretical attention has been paid to this phenomenon, and the generally accepted explanations are that the equatorial orientation has unfavorable dipole–dipole interactions[1,12,15,20,21] and that hyperconjugative delocalization of ring oxygen lone pair density into the *anti* exocyclic $\sigma^*_{C(1)-O}$ orbital stabilizes the axial anomer.[16–19,22,23] This hyperconjugative stabilization has been found to be quite general in a wide variety of systems not limited to O–C–O–R linkages.[24] Attempts to calculate the anomeric effect should take account of the relatively large changes in bond lengths and angles that accompany reorientation of the anomeric bond and internal rotations.[16,18,19,25] Molecular orbital calculations give mixed results on whether the axial or equatorial orientation is preferred in simple, unsubstituted sugars.[11,16,26] Given the observed[12,16] 64:36 equatorial:axial aqueous equilibrium in glucose, it is thus not clear whether the equatorial anomer predominates because of improved solvation or whether the gas-phase potential is responsible. Lemieux and co-workers[1,21,27] inferred by NMR that hydroxylic solvation opposes the anomeric effect. Improved aqueous solvation of the equatorial anomer has been inferred theoretically for both simple pyranoses[16,20,26,28] and their derivatives.[23,29] Different conclusions have been drawn, however, on the question of whether the supposed differential solvation effect involves specific hydrogen bonding interactions[1,20,21,27,28] or is dominated by electrostatic (i.e., electric polarization) effects.[26,29,30]

A recent molecular dynamics simulation by Ha *et al.*[10] using rigid TIP3P[31] water and a CHARMM-type[32] molecular mechanics representation of the solute with fixed O–H and C–H bond distances yielded an aqueous free energy difference $\Delta G°_{aq}$-(β-D→α-D) of -0.3 ± 0.4 kcal/mol (close to the experimental[12] +0.3 kcal/mol). The authors report a large difference in the solvation free energies for the two anomers, with the equatorial being better solvated by 3.0 ± 0.5 kcal/mol. Comparison to an earlier study by Brady,[8] who used the simple-point-charge (SPC)[33] model for water and a sugar potential energy function[34] that favors the equatorial anomer in vacuum, indicates possible sensitivity to the potential energy function or nonbonded truncation method. Nevertheless, Ha *et al.* conclude from the large *magnitude*, if not the precise value, of the calculated solvation difference that the aqueous-phase preference for the equatorial anomer is primarily a hydration effect.

Polavarapu and Ewig[11] have recently calculated the solute energetics by ab initio electronic structure methods. They provided relative energies at the HF/4-31G[35] level of several conformers resulting from anomerism and internal rotation around the C(5)–C(6) and C(6)–O bonds. They found the conformers illustrated in Figure 1 to be the lowest in energy for the two anomers. Polavarapu and Ewig[11] found, for the $\bar{G}$ isomer, that HF/4-31G and HF/6-31G*//HF/4-31G[35] calculations yield β-D→α-D gas-phase free energy differences of -1.6 and -0.4 kcal/mol, respectively.

In another relevant study, Homans[36] concluded that inclusion of solvent water is *necessary* for an adequate representation of the available conformational space in simulations of oligosaccharides.

We present in this paper a quantum mechanical/statistical mechanical study using recently developed aqueous solvation models[37–40] to compare a large number of glucose conformations in both the gas phase and aqueous solution, and we place special emphasis on two of these issues. First, is the anomeric equilibrium determined primarily by solvation effects or by effects that also exist in the isolated molecule? Second, how sensitive to solvation are the rotameric conformational equilibria of the hydroxyl groups? Section 2 provides a brief overview of the theoretical methods, and Sections 3 and 4 present results and discussion. Section 3 addresses the issues of anomeric equilibrium and hydroxymethyl conformation, and Section 4 explores the relative stability of various rotamers of the remaining hydroxyl groups for one hydroxymethyl conformer of the α-D anomer. Section 5 provides concluding remarks.

(17) (a) Lucken, E. A. C. *J. Chem. Soc.* **1959**, 2954. (b) Romers, C.; Altona, C.; Buys, H. R.; Havinga, E. In *Topics in Stereochemistry*; Eliel, E. L., Allinger, N. L., Eds.; Wiley: New York, 1967; Vol. 4, p 39.
(18) Wolfe, S.; Whangbo, M.-H.; Mitchell, D. J. *Carbohydr. Res.* **1979**, *69*, 1.
(19) Kirby, A. J. *The Anomeric Effect and Related Stereoelectronic Effects at Oxygen*; Springer-Verlag: New York, 1983.
(20) Kabayama, M. A.; Patterson, D.; Piche, L. *Can. J. Chem.* **1958**, *36*, 563.
(21) Lemieux, R. U.; Pavia, A. A.; Martin, J. C.; Watanabe, K. A. *Can. J. Chem.* **1969**, *47*, 4427.
(22) (a) Wiberg, K. B.; Murcko, M. A. *J. Am. Chem. Soc.* **1989**, *111*, 4821. (b) Krol, M. C.; C. Huige, J. M.; Altona, C. *J. Comput. Chem.* **1990**, *11*, 765. (c) Hati, S.; Datta, D. *J. Org. Chem.* **1992**, *57*, 6056.
(23) Cramer, C. J. *J. Org. Chem.* **1992**, *57*, 7034.
(24) (a) de Hoog, A. J.; Buys, H. R.; Altona, C.; Havinga, E. *Tetrahedron* **1969**, *25*, 3365. (b) Lemieux, R. U. *Pure Appl. Chem.* **1971**, *25*, 527. (c) Eliel, E. L.; Bailey, W. F. *J. Am. Chem. Soc.* **1974**, *96*, 1798. (d) Schleyer, P. v. R.; Jemmis, E. D.; Spitznagel, G. W. *J. Am. Chem. Soc.* **1975**, *107*, 6393. (e) Reed, A. E.; Schleyer, P. v. R. *J. Am. Chem. Soc.* **1987**, *109*, 7362. (f) Gorenstein, D. G. *Chem. Rev.* **1987**, *87*, 1047. (g) Denmark, S. E.; Cramer, C. J. *J. Org. Chem.* **1990**, *55*, 1806. (h) Cramer, C. J. *J. Am. Chem. Soc.* **1990**, *112*, 7965. (i) Juaristi, E.; Cuevas, G. *Tetrahedron* **1992**, *24*, 5019.
(25) Berman, H. M.; Chu, S. S. C.; Jeffrey, G. A. *Science* **1967**, *157*, 1576.
(26) Tvaroška, I.; Kožár, T. *Theor. Chim. Acta* **1986**, *70*, 99.
(27) Praly, J.-P.; Lemieux, R. U. *Can. J. Chem.* **1987**, *65*, 213.
(28) (a) Tait, M. J.; Suggett, A.; Franks, F.; Ablett, S.; Quickenden, P. A. *J. Solution Chem.* **1972**, *1*, 131. (b) Suggett, A. *J. Solution Chem.* **1976**, *5*, 33. (c) Franks, F. *Pure Appl. Chem.* **1987**, *59*, 1189.
(29) Tvaroška, I.; Kožár, T. *Int. J. Quantum Chem.* **1983**, *23*, 765.
(30) Tvaroška, I.; Kožár, T. *J. Am. Chem. Soc.* **1980**, *102*, 6929.
(31) Jorgensen, W. L. *J. Am. Chem. Soc.* **1981**, *103*, 335.
(32) Brooks, B. R.; Bruccoleri, R. E.; Olafson, B. D.; States, D. J.; Swaminathan, S.; Karplus, M. *J. Comput. Chem.* **1983**, *4*, 187. Ha, S. N.; Field, M.; Giammona, A.; Brady, J. W. *Carbohydr. Res.* **1988**, *180*, 207.
(33) Berendsen, H. J. C.; Postma, J. P. M.; van Gunsteren, W. F.; Hermans, J. In *Intermolecular Forces*; Pullman, B., Ed.; Reidel: Dordrecht, The Netherlands, 1981; p 331.
(34) Rasmussen, K. *Acta Chem. Scand.* **1982**, *A36*, 323.
(35) For details of this notation and references for the basis sets employed, see: Hehre, W. J.; Radom, L.; Schleyer, P. v. R.; Pople, J. A. *Ab Initio Molecular Orbital Theory*; Wiley: New York, 1986.
(36) Homans, S. W. *Biochemistry* **1990**, *29*, 9110.
(37) Cramer, C. J.; Truhlar, D. G. *J. Am. Chem. Soc.* **1991**, *113*, 8305, 9901(E).
(38) Cramer, C. J.; Truhlar, D. G. *Science* **1992**, *256*, 213.
(39) Cramer, C. J.; Truhlar, D. G. *J. Comput. Chem.* **1992**, *13*, 1089.
(40) Cramer, C. J.; Truhlar, D. G. *J. Comput.-Aided Mol. Des.* **1992**, *6*, 629.

2. Computational Methods

Gas-phase energies E_g were modeled by neglect of diatomic differential overlap (NDDO)[41] molecular orbital theory, employing both the Austin Model 1 (AM1)[42] and parametrized Model 3 (PM3)[43] Hamiltonians. In order to calculate solvation free energies, the AM1-SM2,[38] PM3-SM3,[39] and AM1-SM1a[37] aqueous solvation models were applied with a standard state of 1 M in both the gas phase and aqueous solution. These models incorporate continuum solvent polarization effects directly into the Fock matrix of the solute NDDO calculation, and they include first hydration shell effects via a surface tension term. The resulting free energies of solvation, $\Delta G°_S$, may be partitioned into (i) a term, ΔG_{ENP}, which includes the effects of electric polarization of the solvent and the associated solvent-induced electronic and nuclear relaxation of the solute and (ii) a term, $G°_{CDS}$, which accounts for solvent-accessible-surface-area effects like cavitation, dispersion, and local modification of the water structure, e.g., hydrophobic structural changes and hydrophilic hydrogen bonding. We note that in the ENP term the solute is represented as a set of distributed monopoles (i.e., atomic charges on *every* atom), and in the CDS term it is represented by a cavity boundary passing through the first hydration shell of the continuum solvent. Further details of the SMx models are reviewed elsewhere.[40]

The aqueous free energies are then appoximated by

$$G°_{aq} = G°_g + \Delta G°_S \tag{1}$$

where the gas-phase free energy is

$$G°_g = E_g + G°_{trans}(g) + G_{rot}(g) + G_{vib}(g) \tag{2}$$

where E_g is the gas-phase electronic energy, including nuclear repulsion, and $G°_{trans}(g)$, $G_{rot}(g)$, and $G_{vib}(g)$ are the gas-phase translational, rotational, and vibrational free energy, respectively. E_g is taken either from the present AM1 or PM3 calculations or an ab initio level as described below. $G°_{trans}(g)$, $G_{rot}(g)$, and $G_{vib}(g)$ are taken from the HF/4-31G calculations of ref 11. All free energies refer to a temperature of 298 K. All E_g and $G°_g$ values are calculated at gas-phase optimized structures, and $\Delta G°_S$ is calculated at the AM1-SM2, PM3-SM3, or AM1-SM1a level by re-optimization in solution.

Figure 1 illustrates the conformers of the α-D and β-D anomers studied in Section 3. The illustrated counterclockwise array of hydrogen bonds resulting from the conserved orientation of the non-anomeric ring hydroxyls (when viewed from above) was deemed to represent the minimum energy arrangement of these groups for each hydroxymethyl conformer. This is supported by the results presented in Section 4. Each structure in Figure 1 is a minimum-energy gas-phase conformer optimized by the AM1 method. For the aqueous-phase calculations, each structure was re-optimized with solvent present.

In Section 4, the hydroxymethyl group was chosen to be *G* (and remained so in every optimization) while all 81 (3^4) possible rotamers of the remaining four hydroxyl groups were fully optimized at both the AM1 and PM3 levels. A total of 26 rotamers were stationary in both models, 7 were stationary only in AM1, 14 were stationary only in PM3, and 34 were not stationary in either model.

All optimizations were carried out with the BFGS algorithm.[44] Since the BFGS algorithm minimizes the total energy, and all of these stationary points are of C_1 symmetry, we assume that they are all minima. Each of the gas-phase stationary points were reoptimized with the appropriate SMx model to find the optimum aqueous structure.

All computations were performed with a pre-release version of the computer program AMSOL-version 3.0.1c, which is now available from QCPE.[45] The AMSOL program is based on AMPAC-version 2.1.[46] All geometry optimizations employed the PRECISE criteria of the program. SCF convergence tolerances were set to 10^{-7} and 10^{-6} for gas-phase and solution calculations, respectively.

Table I. Relative Energies and Free Energies (kcal/mol) for Glucose Conformers[a]

	E_g			$G°_g$		$G°_{aq}$(eq 1)		
structure	AM1	4-31G	6-31G*	4-31G	6-31G*	AM1	4-31G	6-31G*
α-D-$\bar{G}$	0.5	0.3	0.3	0.0[b]	0.0[b]	0.9	0.2	0.2
α-D-*T*	0.0[b,c]	0.0[b]	0.0[b]	0.0	0.0	0.9	0.4	0.4
α-D-*G*	0.1	0.7	0.7	0.2	0.2	0.0[b]	0.0[b]	0.0[b]
α-D(av)[d]				−0.6	−0.6	−0.2	−0.5	−0.5
β-D-$\bar{G}$	2.9	2.5	1.3	1.6	0.4	2.8	1.8	0.6
β-D-*T*	1.9	2.5	1.3	1.8	0.6	2.1	2.1	0.9
β-D-*G*	2.6	3.2	1.0	2.1	0.9	1.8	1.8	0.6
β-D(av)[d]				1.1	−0.1	1.4	1.2	0.0

[a] Each entry is referenced to the lowest conformer free energy in its column. All solvation energies in this table are calculated by the AM1-SM2 method, and all gas-phase translational, rotational, and vibrational free energies are taken from the HF/4-31G calculations of ref 11; the second row of each column heading is an abbreviation for the origin of the gas-phase electronic energy data, as explained in Section 3. [b] Lowest value in column; zero by convention. [c] AM1 heat of formation is −303.59 kcal/mol. All other AM1 heats of formation may be derived from this value. [d] Conformational average from eq 3.

3. Anomeric and Hydroxymethyl Equilibria

Calculated structures are similar at the AM1 and HF/4-31G levels; each of the conformers shown in Figure 1 is also predicted to be a local minimum at the HF/4-31G level.[11] This is in accord with the results of Ferguson *et al.*,[47] who observed a good correlation between AM1 and Hartree–Fock predictions for the structures of alicyclic six-membered rings.

The present AM1 gas-phase energies are summarized and compared to the ab initio results[11] in Table I. We use the abbreviation 4-31G for HF/4-31G and the abbreviation 6-31G* for values obtained by correcting the individual conformer HF/4-31G values by the HF/6-31G*//HF/4-31G single-point-energy difference calculated[11] for the $\bar{G}$ conformers of the α-D and β-D anomers. Overall, the AM1 relative gas-phase energies for the six glucose conformers agree remarkably well with the 4-31G results; in every case, AM1 puts the α-D anomer lower in energy than the β-D by 1.9–2.5 kcal/mol. However, the 6-31G* calculations predict less preference for α-D in the gas phase. (The effect of electron correlation on ab initio predictions of the conformations of vicinal hydroxyl groups has been studied only for dioses so far.[48])

The AM1 results are similar to the ab initio calculations of Wiberg and Murcko[22a] on methyl glucopyranoside, where the axial anomer was found to be 2.1 kcal/mol more stable than the equatorial, but Ha *et al.*[10] found a gas-phase molecular mechanics energy difference of only 0.7–0.9 kcal/mol for glucose, again with axial lower in energy, which is closer to the 6-31G* value than to the AM1 or 4-31G.

Table I also shows the ab initio $G°_g$ values; those denoted 4-31G are from the HF/4-31G calculations,[11] and those denoted 6-31G* are from 6-31G* E_g values combined with HF/4-31G calculations for the nuclear motion contributions. Further insight on this question is provided by calculating a $\Delta G°_g$ value from the ab initio calculations. This is accomplished by averaging over the three conformations ($C = \bar{G}, T, G$) for a given anomer as follows:

$$\exp[-G°_g(\beta \text{ or } \alpha)/RT] = \sum_C \exp[-G°_g(\beta C \text{ or } \alpha C)/RT] \tag{3}$$

(41) Pople, J. A.; Santry, D. P.; Segal, G. A. *J. Chem. Phys.* **1965**, *43*, S129.
(42) Dewar, M. J. S.; Zoebisch, E. G.; Healy, E. F.; Stewart, J. J. P. *J. Am. Chem. Soc.* **1985**, *107*, 3902.
(43) Stewart, J. J. P. *J. Comp. Chem.* **1989**, *10*, 209, 221. Stewart, J. J. P. *J. Comput.-Aided Mol. Des.* **1990**, *4*, 1.
(44) (a) Broyden, C. G. *J. Inst. Mathem. Appl.* **1970**, *6*, 222. (b) Fletcher, R. *Comput. J.* **1970**, *13*, 317. (c) Goldfarb, D. *Math. Comput.* **1970**, *24*, 23. (d) Shanno, D. F. *Math. Comput.* **1970**, *24*, 647.
(45) Cramer, C. J.; Lynch, G. L.; Truhlar, D. G. QCPE program 606-version 3.0.1c, Quantum Chemistry Program Exchange, Chemistry Department, Indiana University, Bloomington, IN, 1992; *QCPE Bull.* **1993**, *13*, 9.
(46) Liotard, D. A.; Healy, E. F.; Ruiz, J. M.; Dewar, M. J. S. *QCPE Bull.* **1989**, *10*, 86.
(47) Ferguson, D. M.; Gould, I. R.; Glauser, W. A.; Schroeder, S.; Kollman, P. A. *J. Comput. Chem.* **1992**, *13*, 525.
(48) (a) Barzaghi, M.; Gamba, A.; Morosi, G. *Theochem.* **1988**, *170*, 69. (b) Cabral, B. J. C.; Albuquerque, L. M. P. C.; Fernandes, F. M. S. S. *Theor. Chim. Acta* **1991**, *78*, 271. (c) Park, C. G.; Tasumi, M. *J. Phys. Chem.* **1991**, *95*, 2757.
(49) Cramer, C. J.; Truhlar, D. G. *J. Am. Chem. Soc.* **1991**, *113*, 8552, 9901(E).

Table II. AM1-SM2 Absolute Free Energies of Solvation (kcal/mol) for Glucose Conformers

structure	ΔG_{ENP}	ΔG°_{CDS}	ΔG°_S
α-D-$\bar{G}$	−0.8	−17.0	−17.8
α-D-T	−0.8	−16.8	−17.6
α-D-G	−0.7	−17.5	−18.1
β-D-$\bar{G}$	−0.4	−17.3	−17.7
β-D-T	−0.5	−17.1	−17.6
β-D-G	−0.4	−17.8	−18.2

where R is the gas constant, and T is temperature. Then

$$\Delta G^\circ_g(\beta\rightarrow\alpha) = G^\circ_g(\beta) - G^\circ_g(\alpha) \quad (4)$$

This average yields $\Delta G^\circ_g(\beta\text{-D}\rightarrow\alpha\text{-D}) = -1.7$ kcal/mol at the 4-31G level and −0.5 kcal/mol at the 6-31G* level. These values are less negative than the $\Delta E_g(\beta\rightarrow\alpha)$ values for the lowest energy conformers (−2.5 and −1.0 kcal/mol at these respective levels). The 6-31G* value of $\Delta G^\circ_g(\beta\text{-D}\rightarrow\alpha\text{-D}) = -0.5$ kcal/mol is in good agreement with the value of −0.7 kcal/mol calculated by Tvaroška and Kožár by conformational averaging of semiempirical E_g[26] values. Ha *et al.* found a more substantial intramolecular β-D→α-D free energy difference of −3.6 kcal/mol in solution. (Combining this with the solvation difference of 3.0 kcal/mol would lead to a difference in G°_{aq} of −0.6 kcal/mol, but further averaging without component analysis yielded their final value of −0.3 ± 0.4 kcal/mol.) Ha *et al.* concluded from the large difference between the intramolecular contribution (−3.6 kcal/mol) to the β-D→α-D free energy change in solution and the difference (−0.7 to −0.9 kcal/mol) they calculated for the energy minima in vacuum that a dynamic average in solution is required to obtain a meaningful result. The $\Delta G^\circ_{aq}(\beta\text{-D}\rightarrow\alpha\text{-D}) - \Delta E_g(\beta\text{-D}\rightarrow\alpha\text{-D})$ difference reported by Ha *et al.*[10] [3.6 − (−0.9) kcal/mol] is not only larger in magnitude than the gas-phase ab initio result of Polavarapu and Ewig[11] for $\Delta G^\circ_g(\beta\text{-D}\rightarrow\alpha\text{-D}) - \Delta E_g(\beta\text{-D}\rightarrow\alpha\text{-D})$, but it is in the opposite direction, implying a remarkable solvation shift.

The SMx models, by their semiempirical nature, include all solvation effects in ΔG°_S, and so eq 1, with aqueous conformational averaging of the 6-31G* vacuum results analogous to eq 3 for the first term on the right-hand side and the AM1-SM2 model for the second term, provides our best estimate. These results are shown in the last columns of Table I. Our final value for the solvation effect on the free energy change accompanying the mutarotation is the difference between the −0.5 kcal/mol β→α free energy difference in the last column of Table I and the −0.5 kcal/mol free energy difference in the fourth last column. That is, *we predict no solvation effect on the* β-D→α-D *free energy difference.*

Table II gives the SM2 solvation energies, and it shows that the SM2 models, which do not suffer from the assumption[10] that the atomic charges are the same in the α and β anomers, nevertheless do not favor either of the α and β anomers to any appreciable extent. The absolute free energies of solvation for the various conformers of the α and β anomers are provided in Table II, while the relative free energies in aqueous solution are given in Table I. Experimental solvation free energy values for glucose are not available, and there do not appear to be any previously calculated absolute free energies of solvation to which to compare. It is noteworthy and encouraging, however, that similar values are obtained for identical isomers with both the PM3–SM3 and AM1–SM1a solvation models, as will be discussed in Section 4. We have shown[37-40,49] in several cases that the errors in solvation free energies due to using the SMx models are about an order of magnitude smaller than the errors in the gas-phase heats of formation calculated by the AM1 and PM3 solute Hamiltonians.

Our final calculated value for $\Delta G^\circ_{aq}(\beta\text{-D}\rightarrow\alpha\text{-D})$ is −0.5 kcal/mol (which may be compared to the experimental[12] value of +0.3 kcal/mol). More important than the 0.8 kcal/mol quantitative discrepancy is the picture we obtain, which is quite different from the previous one.[10] We find that solvation effects cancel out on the anomeric equilibrium, so it is dominated by effects present in the vacuum calculation. A critical difference between our calculations and the recent molecular dynamics simulations may be the fact that the molecular dynamics simulations employed a potential energy function[32] in which hydrogen bonding was modeled by increasing the atomic charges. Mimicking the specific, but somewhat orientation-independent OH hydrogen bonding interactions by the more differentiating electrostatic terms may overestimate the solvation effect on the anomeric equilibrium. If we accept as our final estimate that solvation has no effect on the mutarotation free energy difference and the best estimate (+0.6 kcal/mol from Table I for any rotamer) of the mutarotation change in rotational and vibrational free energy, then using

$$\Delta G^\circ_{aq}(\beta\rightarrow\alpha) = \Delta E_g(\beta\rightarrow\alpha) + [\Delta G_{rot}(\beta\rightarrow\alpha) + \Delta G_{vib}(\beta\rightarrow\alpha)] + \Delta\Delta G^\circ_S(\beta\rightarrow\alpha) \quad (5)$$

and the experimental $\Delta G^\circ_{aq}(\beta\text{-D}\rightarrow\alpha\text{-D})$ of +0.3 kcal/mol we find that $\Delta E_g(\beta\text{-D}\rightarrow\alpha\text{-D})$ is −0.3 kcal/mol. That is, the gas-phase anomeric energy difference, without nuclear motion corrections, is 0.3 kcal/mol in favor of axial; this is quite reasonable, considering earlier estimates of 2.5,[11] 1.3,[11] and 0.8[10] kcal/mol in the same direction and that inclusion of higher levels of electronic correlation would probably further lower the middle value, which is the one we used. If we used the gas-phase value of ref 10, the discrepancy from experiment would be only 0.3 kcal/mol.

We find that solvation does play a discriminating role, however, in determining the conformation of the hydroxymethyl group. Thus, when we add the AM1-SM2 solvation free energies to the ab initio gas-phase free energies, we find the $\bar{G}$ and G conformers to be lower in energy than the T for both anomers, in agreement with experiment.[13] In both anomers, the G arrangement is significantly better solvated than either of the other two possibilities. Our results in this respect are consistent with the glucose simulations of Ha *et al.*[10] and the methyl-D-glucoside simulations of Kroon-Batenburg and Kroon[3] (who used SPC[33] water and a solute potential[50] that treated CH and CH_2 groups as united atoms and favors G over T by 2.7 kcal/mol) since both groups observed that *trans* converted to *gauche* in every case, but only one *gauche*-to-*trans* conversion was observed.

We present a detailed discussion of the breakdown of ΔG°_S into ΔG_{ENP} and G°_{CDS} in Section 4. Some comment on the breakdown as it affects the anomeric equilibrium is relevant here though, and in particular we note and discuss the facts, shown in Table II, that ΔG°_S is dominated by G°_{CDS}, which is insensitive to atomic charges in our model, and that the ENP and CDS terms partially cancel in the solvation effect on the anomeric equilibrium.

The dominance of ΔG°_S by G°_{CDS} is due primarily to hydrophilic interactions of the hydroxyl groups with the first solvent shell. The SMx models predict a similar dominance of the G°_{CDS} term in alcohols, diols, and carboxylic acids, for which the predicted net free energies of solvation are in good agreement with experiment.[37-40] This indicates reasonable reliability for the predictions of the SMx models in this regard.

The net small value of ΔG_{ENP} results from the near cancellation of several sizable, mutually interacting bond dipoles, which makes it hard to single out any one dominant charge contribution. In particular, although the optimized aqueous atomic charges vary by up to 0.05 (in the usual units of the charge of an electron) for the six conformers in Table II, the effect of the various conformational differences may be to either increase or decrease the net solvation energy depending on the proximity of each charge to other like or unlike charges. Thus for many individual atoms,

(50) Koehler, J.; Saenger, W.; Van Gunsteren, W. F. *Eur. Biophys. J.* **1987**, *15*, 197.

the change in their contribution to the ΔG_{ENP} term from one conformer to another is often larger than the net change for the whole molecule, making the attempt to provide a simple discussion futile. The only obvious trend for the hydroxymethyl conformers is that ΔG_{ENP} tends to be 0.3–0.4 kcal/mol more negative for the α-D anomers than for the β-D anomers. This effect offsets the more intuitively obvious trend in $G°_{CDS}$ for the anomeric equilibrium (i.e., that $G°_{CDS}$ is more negative for the β-D anomer with its more exposed equatorial OH). The partial cancellation of these two effects results in the small net difference in free energies of solvation of the two anomers in the present calculation. (Since the small difference results from a partial cancellation rather than from the two terms being individually small, the cancellation can be less complete in other solvents, and so the present result is not inconsistent with the experimental result[1] that there are different anomeric ratios in different solvents. We also note that the solvent dependence is slight in kilocalorie units.)

Table I indicates that the *G* conformer is better solvated than the others by about 0.5 kcal/mol for both anomers, and Table II shows that this is due to the $G°_{CDS}$ term. Thus the $G°_{CDS}$ term dominates not only the net solvation free energy but also the hydroxymethyl conformational difference in the free energies. Furthermore, this difference derives almost entirely from the C(6) hydroxyl group, in excellent agreement with the conclusions of Kroon-Batenburg and Kroon based upon their explicit water simulations. This is a dramatic confirmation that our continuum treatment of solute–solvent interactions can reproduce even subtle features of explicit water simulations. The convenience of the continuum treatment can then be exploited to systematically explore a wide range of interesting conformational issues, as is done in Section 4.

4. Hydroxyl Rotamers

The rotamers listed in Figure 1 all have a counterclockwise cyclic internal array of hydrogen bonds. While it is intuitively reasonable to assume that this arrangement of the ring hydroxyl groups is favored over others, a thorough quantum chemical comparison of the various possibilities has not previously been reported. Some attention has been paid to rotamers in which the hydrogen bonding array is reversed (i.e. clockwise) and to a few disrupted hydrogen bonding networks.[11,51,52] Experimental evidence has been presented for cooperative hydrogen bond conjugation,[53] and it has also been inferred that a cyclic (clockwise) array of H bonds is stable enough to be manifested in isotope shift ^{1}H NMR resonances in glucose in the dipolar aprotic solvent $(CD_3)_2SO$.[54] In recent explicit-water simulations of maltose (which is a glucose disaccharide), Brady and Schmidt[55] found that adjacent hydroxyl groups on both rings made hydrogen bonds to one another for extended periods. In other related work, Zheng et al.[56] have argued that consecutive intramolecular hydrogen bonds seen in saccharide simulations are artifacts of incorrect force fields. No prior study has systematically examined the effect of solvation on the rotameric equilibria of any saccharide.

To do so, we have focused on the 81 possible C(1)–C(4) rotamers of the *G* conformer of the α-D anomer. On the basis of both the gas-phase and solution data in Table I, the α-D-*G* rotamer pictured in Figure 1 is likely the global minimum structure for glucose. In order to discuss these conformers, it is convenient to employ a shorthand notation which defines all of the four ring hydroxyl rotamers. We employ a four-letter descriptor, e.g., $g\bar{g}\bar{g}g$, where the order of the letters corresponds to the hydroxyl groups at C(1), C(2), C(3), and C(4), respectively. Each letter indicates whether the H–O–C(n)–C(n–1) dihedral angle (or the H–O–C(1)–O dihedral for the anomeric hydroxyl) is *gauche*(–) [$\bar{g}$], *anti* [*t*], or *gauche*(+) [*g*]. Our convention is to define *gauche*(–) as indicating that a counterclockwise [viewed in the O-to-C(n) direction] rotation of the OH group of approximately 60° is required to eclipse the bond to the C(n–1) or ring O, while for *gauche*(+) the rotation is clockwise. The convention for labeling

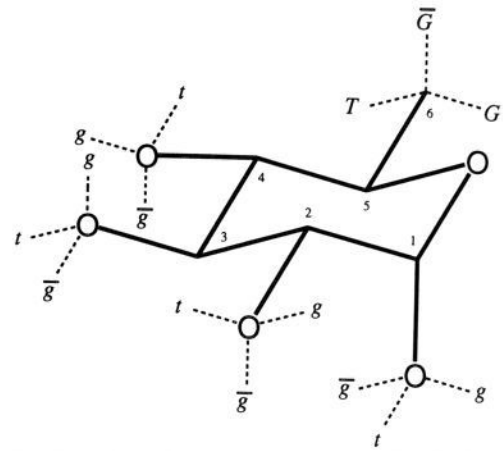

Figure 2. Illustration of the conventions for numbering the ring and the exocyclic carbon and for labeling the rotamers of α-D-glucose.

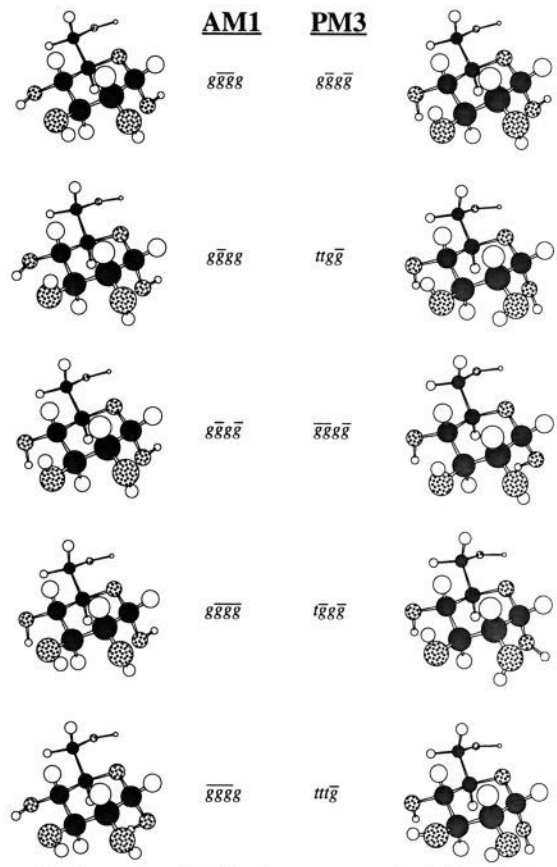

Figure 3. Illustration of the five lowest-energy ring hydroxyl rotamers found for the *G* hydroxymethyl conformer of α-D-glucose at the AM1 and PM3 levels.

(51) French, A. D.; Rowland, R. S.; Allinger, N. L. In *Computer Modeling of Carbohydrate Molecules*; ACS Symp. Ser. No. 430; French, A. D., Brady, J. W., Eds.; American Chemical Society: Washington, DC, 1990.
(52) Various hydrogen bonding networks have also been examined in ketopyranoses at the AM1 level: (a) Woods, R. J.; Szarek, W. A.; Smith, V. H., Jr. *J. Am. Chem. Soc.* **1990**, *112*, 4732. (b) Woods, R. J.; Szarek, W. A.; Smith, V. H., Jr. *Can. J. Chem.* **1991**, *69*, 1917.
(53) Lemieux, R. U.; Pavia, A. A. *Can. J. Chem.* **1969**, *47*, 4441.
(54) Christofides, J. C.; Davies, D. B. *J. Chem. Soc., Perkin Trans 2* **1987**, 97. See also: Christophides, J. C.; Davies, D. B.; Martin, J. A.; Rathbone, E. B. *J. Am. Chem. Soc.* **1986**, *108*, 5738.
(55) Brady, J. W.; Schmidt, R. K. *J. Phys. Chem.* **1993**, *97*, 958.
(56) Zheng, Y.-J.; Le Grand, S. M.; Merz, K. M., Jr. *J. Comput. Chem.* **1992**, *13*, 772.
(57) Lemieux, R. U.; Koto, S. *Tetrahedron* **1974**, *30*, 1933.
(58) (a) Tse, Y.-C.; Newton, M. D. *J. Am. Chem. Soc.* **1977**, *99*, 611. (b) Jeffrey, G. A.; Lewis, L. *Carbohydr. Res.* **1978**, *60*, 179.

Table III. Relative AM1 and AM1-SM2 Energies[a] for α-D-*G* Glucose Conformers

isomer	AM1[b]	AM1-SM2[c]	C(1)–OH[d]	C(2)–OH[d]	C(3)–OH[d]	C(4)–OH[d]
g$\bar{g}$$\bar{g}$g	0.00	0.00	**	*cc*	*cc*	*cc*
g$\bar{g}$gg	0.73	0.37	**	*cc*		*cc*
g$\bar{g}$g$\bar{g}$	0.96	0.35	**	*cc*		
g$\bar{g}$$\bar{g}$$\bar{g}$	1.19	0.70	**	*cc*	*cc*	
$\bar{g}$$\bar{g}$$\bar{g}$g	1.35	0.78	*	*cc*	*cc*	*cc*
g$\bar{g}$t$\bar{g}$	1.41	0.82	**	*cc*	*c*	
ttt$\bar{g}$	2.43	2.08	*c*	*c*	*c*	
g$\bar{g}$tt	2.85	2.24	**	*cc*	*c*	
$\bar{g}$$\bar{g}$$\bar{g}$$\bar{g}$	2.94	1.98	*	*cc*	*cc*	
ttg$\bar{g}$	2.96	2.50	*c*	*c*		
gtt$\bar{g}$	2.97	2.39	**	*c*	*c*	
$\bar{g}$$\bar{g}g\bar{g}$	3.10	1.76	*	*cc*		
$\bar{g}$$\bar{g}t\bar{g}$	3.65	2.35				
tttt	4.00	3.62	*c*	*c*	*c*	
ttgg	4.00	3.73	*c*	*c*		*cc*
g$\bar{g}$gt	4.06	3.08	**	*cc*		
$\bar{g}$ttt	4.35	3.43	*	*c*	*c*	
t$\bar{g}$g$\bar{g}$	4.39	3.65				
$\bar{g}$$\bar{g}$tt	4.47	3.15	*	*cc*	*c*	
$\bar{g}$tgg	4.53	3.58	*	*c*		*cc*
gttt	4.55	3.98	**	*c*	*c*	
t$\bar{g}$t$\bar{g}$	4.63	3.84			*c*	
$\bar{g}$gt$\bar{g}$	5.02	4.21	*		*c*	
$\bar{g}$ggg	5.24	3.97	*			
tttg	5.29	4.87	*c*	*c*		
gttg	5.54	4.86	**	*c*		
gt$\bar{g}$g	5.55	4.92	**			*cc*
$\bar{g}$$\bar{g}$gt	5.56	3.88	*	*cc*		
tt$\bar{g}$g	5.66	4.92	*c*			*cc*
$\bar{g}$ttg	5.71	4.75	*	*c*		
$\bar{g}$t$\bar{g}$g	5.80	4.68	*			*cc*
$\bar{g}$gtt	6.18	5.08	*		*c*	
$\bar{g}$ggt	7.93	6.43	*			

[a] kcal/mol. [b] AM1 gas-phase energies at the gas-phase stationary point. [c] AM1-SM2 free energies of solvation added to AM1 heats of formation at the aqueous stationary point. [d] As explained in Section 4, * and ** denote exo-anomeric effects, and *c* and *cc* denote clockwise and counterclockwise (as viewed from above the ring) intramolecular hydrogen bonds.

Table IV. Relative PM3 and PM3-SM3 Energies (kcal/mol) for α-D-*G* Glucose Conformers

isomer	PM3	PM3-SM3	isomer	PM3	PM3-SM3
g$\bar{g}$$\bar{g}$g	0.00	0.00	*ttgg*	2.54	3.01
ttg$\bar{g}$	0.43	0.99	*$\bar{g}$ggg*	2.60	2.00
$\bar{g}$$\bar{g}$$\bar{g}$g	0.67	0.22	*t$\bar{g}$gt*	2.62	2.44
t$\bar{g}$g$\bar{g}$	0.76	0.96	*$\bar{g}$$\bar{g}$tt*	2.78	2.26
ttt$\bar{g}$	0.85	1.62	*t$\bar{g}$tt*	2.83	2.93
g$\bar{g}$gg	1.11	1.21	*$\bar{g}$g$\bar{g}$g*	3.10	2.83
$\bar{g}$$\bar{g}$gg	1.33	0.95	*$\bar{g}$tgg*	3.15	2.88
g$\bar{g}$t$\bar{g}$	1.45	1.62	*$\bar{g}$g$\bar{g}$$\bar{g}$*	3.18	2.87
g$\bar{g}$$\bar{g}$g	1.53	2.15	*g$\bar{g}$$\bar{g}$t*	3.21	2.96
g$\bar{g}$$\bar{g}$$\bar{g}$	1.57	1.68	*$\bar{g}$$\bar{g}$$\bar{g}$t*	3.32	2.65
tttt	1.64	2.43	*$\bar{g}$gt$\bar{g}$*	3.44	2.91
$\bar{g}$$\bar{g}$$\bar{g}$g	2.04	1.85	*$\bar{g}$ggg*	3.73	2.97
t$\bar{g}$t$\bar{g}$	2.18	2.17	*tg$\bar{g}$$\bar{g}$*	3.73	3.78
g$\bar{g}$gt	2.21	1.83	*$\bar{g}$gtt*	3.75	3.43
$\bar{g}$$\bar{g}$$\bar{g}$$\bar{g}$	2.22	1.94	*$\bar{g}$g$\bar{g}$t*	4.16	3.65
t$\bar{g}$gg	2.22	2.28	*$\bar{g}$ggt*	4.31	3.70
ttgt	2.23	2.59	*ggt$\bar{g}$*	5.33	4.97
$\bar{g}$$\bar{g}$gt	2.29	1.44	*gttg*	5.52	5.42
$\bar{g}$$\bar{g}t\bar{g}$	2.37	1.91	*gt$\bar{g}$g*	5.57	5.47
g$\bar{g}$tt	2.44	2.48	*ggtt*	6.33	6.10

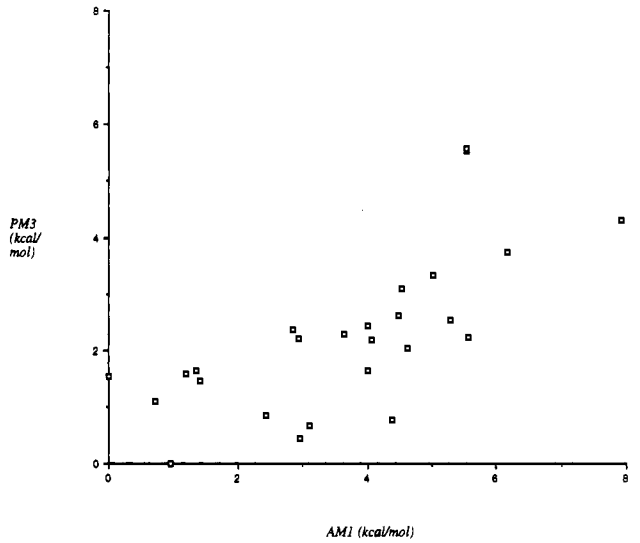

Figure 4. Plot of the AM1 and PM3 relative gas-phase energies (kcal/mol) for the 26 stereostructures that are minima on both surfaces.

the dihedral angles is shown graphically in Figure 2, and the five lowest-energy structures found with either the AM1 or PM3 Hamiltonians are illustrated in Figure 3 to assist in visualization.

Of the 81 possible distinct α-D-*G* rotamers, 33 are predicted to be stationary with the AM1 Hamiltonian and 40 with the PM3. Of these, 26 are common to both. Rotamers not predicted to be stationary converge smoothly to one of the many which are. Table III lists the AM1 minima, ranked in order of increasing gas-phase relative energy. Notice that six are within 2 kcal/mol of the global minimum, and three are within 1 kcal/mol. The AM1 gas-phase relative energies for these rotamers are not expected to be quantitatively accurate. As an example of the differences that might arise at this level of theory, we note that the *g$\bar{g}$tt* rotamer is predicted[11] to be 6.7 and 4.8 kcal/mol higher than the *g$\bar{g}$$\bar{g}$g* at the HF/4-31G//HF/4-31G and HF/6-31G*//HF/4-31G levels,[35] respectively, whereas the AM1 and PM3 results in Table III yield 2.8 and 2.4 kcal/mol, respectively, for this energy difference. However, the goal of this section is to identify trends in solvation free energies among these rotamers and not to predict absolute gas-phase energy differences.

Does solvation "flatten the landscape"? The relative energies of the rotamers upon inclusion of aqueous solvation free energy, calculated by reoptimization at the AM1-SM2 level, are also provided in Table III, and these values show that the answer is yes; with solvent there are eight rotamers within 2 kcal/mol of the global minimum and six within 1.

Table IV provides the same information for the PM3 and PM3-SM3 models. Table V lists the absolute free energies of solvation for the various rotamers calculated via both techniques and decomposed into ΔG_{ENP} and G°_{CDS} terms. Figure 4 is a plot of AM1 vs PM3 calculated relative energies for all common rotamers, while Figure 5 plots the AM1-SM2 vs the PM3-SM3 absolute free energies of solvation for these same structures.

The AM1 data agree with the HF/4-31G calculations of Polavarapu and Ewig[11] insofar as the *g$\bar{g}$$\bar{g}$g* rotamer is predicted to be of lowest energy. This agreement, together with the ability of the AM1-SM2 solvation model to explain the hydroxymethyl conformational preferences (as discussed above), makes it interesting to examine more carefully some of the trends found in the AM1 and AM1-SM2 data. Thus, Table III provides an analysis of the stabilizations afforded to the various rotamers by the anomeric effect and hydrogen bonding at each ring hydroxyl group.

The anomeric hydroxyl group has the opportunity to take advantage of the exocyclic oxygen lone pair delocalization into the endocyclic σ^*_{C-O} bond orbital. This may occur for either the *g* or $\bar{g}$ orientations of the hydroxyl group. The tendency for the *gauche* rotamer of the O–C(1)–O–H dihedral to be preferred as a result of this stabilization is known as the exo-anomeric effect.[1,16,18,19,27,30,57] Alternatively, while the *t* conformation does not permit exo-anomeric stabilization, it does allow hydrogen bonding to the C(2) hydroxyl group, provided this latter hydroxyl is not itself in the $\bar{g}$ conformation. These three possibilities for C(1)–OH (*g*, $\bar{g}$, and *t* where the C(2)–OH is not $\bar{g}$) are indicated by **, *, and *c*, respectively in the C(1)–OH column of Table

Table V. Absolute Free Energies (kcal/mol) of Solvation for α-D-*G* Glucose Rotamers[a]

	AM1-SM2			PM3-SM3		
isomer	ΔG_{ENP}	$G°_{CDS}$	$\Delta G°_S$	ΔG_{ENP}	$G°_{CDS}$	$\Delta G°_S$
g̃g̃g̃g̃	−1.53	−17.56	−19.09	−2.67	−16.57	−19.24
g̃g̃g̃t				−2.94	−16.59	−19.53
g̃g̃g̃g	−1.13	−17.57	−18.70	−2.16	−16.61	−18.77
g̃g̃tg̃	−1.82	−17.61	−19.43	−2.75	−16.60	−19.35
g̃g̃tt	−1.78	−17.57	−19.35	−2.72	−16.61	−19.33
g̃g̃gg̃	−1.87	−17.60	−19.47	−2.87	−16.55	−19.42
g̃g̃gt	−2.16	−17.65	−19.81	−3.18	−16.58	−19.76
g̃g̃gg				−2.70	−16.65	−19.35
g̃tg̃g	−1.67	−17.58	−19.25			
g̃ttt	−1.59	−17.46	−19.05			
g̃ttg	−1.57	−17.52	−19.09			
g̃tgg	−1.47	−17.61	−19.08	−2.63	−16.56	−19.19
g̃gg̃g̃				−2.83	−16.42	−19.25
g̃gg̃t				−3.02	−16.46	−19.48
g̃ggg				−2.53	−16.44	−18.97
g̃gtg̃	−1.67	−17.42	−19.09	−2.95	−16.43	−19.38
g̃gtt	−1.93	−17.30	−19.23	−2.88	−16.41	−19.29
g̃ggg̃	−2.06	−17.34	−19.40	−3.16	−16.35	−19.51
g̃ggt	−2.35	−17.28	−19.63	−3.20	−16.38	−19.58
g̃ggg				−2.99	−16.45	−19.44
tg̃tg̃	−1.32	−17.60	−18.92	−2.27	−16.57	−18.84
tg̃tt				−2.32	−16.50	−18.82
tg̃gg̃	−1.27	−17.60	−18.87	−2.26	−16.51	−18.77
tg̃gt				−2.62	−16.51	−19.13
tg̃gg				−2.36	−16.55	−18.91
ttg̃g	−1.02	−17.51	−18.53			
tttg̃	−0.87	−17.61	−18.48	−1.72	−16.48	−18.20
tttt	−1.09	−17.42	−18.51	−1.73	−16.45	−18.18
tttg	−1.01	−17.54	−18.55			
ttgg̃	−1.04	−17.55	−18.59	−1.91	−16.50	−18.41
ttgt				−2.18	−16.42	−18.60
ttgg	−0.86	−17.54	−18.40	−1.90	−16.50	−18.40
tgg̃g̃				−2.49	−16.43	−18.92
gg̃g̃g̃	−1.13	−17.49	−18.62	−2.35	−16.51	−18.86
gg̃g̃t				−2.72	−16.47	−19.19
gg̃g̃g	−0.66	−17.47	−18.13	−1.88	−16.47	−18.35
gg̃tg̃	−1.10	−17.52	−18.62	−2.37	−16.53	−18.90
gg̃tt	−1.40	−17.34	−18.74	−2.38	−16.48	−18.86
gg̃gg̃	−1.24	−17.50	−18.74	−2.44	−16.53	−18.97
gg̃gt	−1.76	−17.35	−19.11	−2.84	−16.48	−19.32
gg̃gg	−1.00	−17.49	−18.49	−2.35	−16.52	−18.87
gtg̃g	−1.21	−17.55	−18.76	−2.63	−16.44	−19.07
gttg̃	−1.04	−17.65	−18.69			
gttt	−1.22	−17.48	−18.70			
gttg	−1.27	−17.54	−18.81	−2.59	−16.48	−19.07
ggtg̃				−2.94	−16.39	−19.33
ggtt				−2.85	−16.35	−19.20

[a] Listed in ranked order, with a precedence of *g̃* before *t* before *g*.

III. It is apparent that in general exo-anomeric stabilization with the hydroxyl hydrogen directed away from the center of the ring is preferred to the alternative exo-anomeric rotamer, where it is essentially under the center of the ring. This is hardly surprising given the unfavorable interactions with axial ring hydrogens expected for this latter exo-anomeric orientation. Comparing *gg̃*– – to *g̃g̃*– – rotamers (the "–" represents any of the three possibilities) indicates the energy difference between the two exo-anomeric possibilities to be roughly 1.5 kcal/mol. Interestingly, if the non-anomeric hydroxyl groups are engaged in a clockwise hydrogen bonding array, the anomeric hydroxyl *prefers to participate in hydrogen bonding* rather than take advantage of exo-anomeric stabilization. Thus, *tttg̃* and *tttt* are preferred over *gttg̃* and *gttt* by about 0.5 kcal/mol in each case. We recall in this context that anomeric hydroxyls are better H-bond donors than non-anomeric hydroxyls.[58] We additionally note that Woods *et al.*[52a] also found that the *t* conformation of the anomeric hydroxyl could be stabilized in gas-phase calculations by hydrogen bonding to the C(2) hydroxyl, competing with the exo-anomeric effect which stabilizes the other two rotamers. The present results show that this hydrogen bonding effect persists in aqueous solution. This may be related to sweetness.[52a]

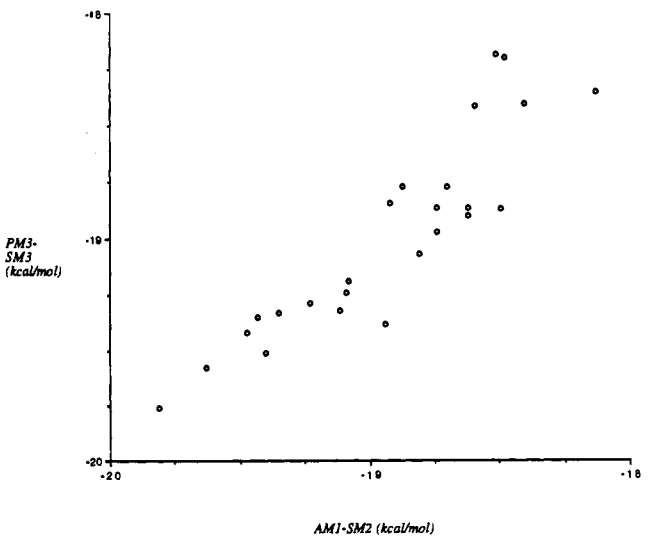

Figure 5. Plot of the AM1-SM2 and PM3-SM3 absolute free energies of solvation (kcal/mol) for the 26 stereostructures that are minima on both surfaces.

The C(2)–OH group may hydrogen bond to either the C(1)–OH (*cc*, for "counterclockwise"—possible for conformers *gg*– – and *g̃g̃*– –, but not *tg̃*– –) or the C(3)–OH (c, for "clockwise"—possible for conformers –*tg*– and –*tt*–, but not –*tg̃*–). The C(3)–OH is in an exactly analogous situation, while the C(4)–OH may only hydrogen bond to the C(3)–OH (*cc*, possible for conformers – –*gg* and – –*g̃g*, but not – –*tg*). These simultaneous interactions are difficult to dissect quantitatively; however, one apparent trend is that in the counterclockwise array, the final C(4)–OH hydrogen bond is worth about 1.3 kcal/mol (e.g., *gg̃g̃g* vs *gg̃g̃g̃*, *g̃g̃g̃g* vs *g̃g̃g̃g̃* and *g̃tgg* vs *g̃ttg*, *ttgg* vs *tttg*). A final interesting point is that whenever the C(3) hydroxyl is hydrogen bonded to the C(2) hydroxyl, the latter is simultaneously hydrogen bonded to the C(1) hydroxyl, i.e. the combination –*gg̃*– does not occur at the AM1 level.

Considering the effects of aqueous solvation, it is apparent that it is relatively insensitive to the rotameric population. Indeed, the variation of about 1.7 kcal/mol across all 33 rotamers is only about 10% of the absolute free energy of solvation. Table V indicates that although the ΔG_{ENP} term is fairly sensitive to rotameric configuration, as might be expected based on the range of the gas-phase dipole moment (from 0.2 D for *gttg̃* to 4.9 D for *ttg̃g*), it is quite a small contributor to the overall $\Delta G°_S$, which is dominated by $G°_{CDS}$. This indicates the predominance of hydrogen bonding interactions at the solvent-accessible OH groups, as discussed in Section 3.

It is of interest that the most poorly solvated conformer is the global minimum, *gg̃g̃g*. This permits the better solvated *gg̃gg* and *gg̃g̃g* rotamers to be brought to within 0.4 kcal/mol, suggesting that they should be considered as non-trivial contributions to the equilibrium mixture. The rotamers *gg̃g̃g̃*, *g̃g̃g̃g*, and *gg̃tg̃* are also within 0.8 kcal/mol of *gg̃g̃g*. We particularly note that two of the five lowest-free-energy rotamers at the AM1-SM2 level, including the favored structure *gg̃g̃g* and also *g̃g̃g̃g*, have consecutive counterclockwise intramolecular hydrogen bonds; two of these five rotamers, namely *gg̃gg* and *gg̃g̃g*, have two of these three hydrogen bonds intact (consecutive ones for *gg̃g̃g̃* and nonconsecutive ones for *gg̃gg*); and the fifth, *gg̃gg̃*, retains one of these intramolecular hydrogen bonds. Thus three of the five lowest-free-energy conformers, including the lowest one, are predicted to maintain consecutive intramolecular hydrogen bonds in aqueous solution by the AM1-SM2 calculations. Two of these three rotamers, plus another showing three consecutive counterclockwise hydrogen bonds, are among the eleven lowest-free-energy rotamers in solution as predicted by the PM3-SM3 model. Furthermore two of the seven lowest-free-energy solution-phase rotamers at the PM3-SM3 level show consecutive clockwise hydrogen bonds, although the lowest-free-energy rotamer at this level shows only one intramolecular hydrogen bond. In summary, our calculations indicate that consecutive intramolecular hydrogen bonds occur in several rotamers liable to be present in aqueous solution in non-negligible amounts, perhaps even in the dominant rotamers. It is interesting to notice, in the context of considering non-lowest but non-negligible rotamers, that the percentage contribution to reactivity or biological activity of the various rotamers may be different than the percentage contributions to the equilibrium mixture.

It is also of some interest to identify particular rotameric combinations which appear to be especially well or poorly solvated; such differential solvation may play a role in other pyranoses too. It appears in general that the combinations *g̃g̃*– –, *g̃g*– –, and – –*gt* are well solvated, while the combinations –*g̃g̃*– and *tt*– – are not.

Kroon-Batenburg and Kroon[3] proposed that the better solvation of *G* vs *T* is due to its having lower-lying rotamers without intraglucose hydrogen bonding. Table III shows, however, that such non-hydrogen-bonded rotamers are *not* the dominant ones in our calculations.

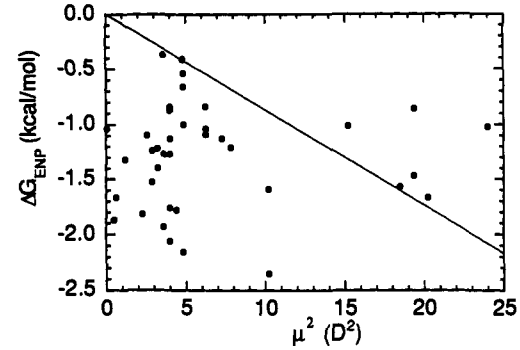

Figure 6. Plot of the AM1-SM2 ΔG_{ENP} values vs the square of the AM1 gas-phase dipole moment for the rotamers listed in Tables II and III. The straight line is the prediction of the Onsager equation.

The observation that rotameric solvation free energies differ primarily in ΔG_{ENP} was explored further. As mentioned in Section 3, the overall molecular dipole moment is a very poor descriptor of the detailed distribution of charge within these molecules. This point is worth emphasizing because of the widespread use of the Onsager dipole-induced reaction-field model for calculating free energies of solvation.[59-61] This model yields

$$\Delta G°_S = -\frac{(\epsilon - 1)\mu^2}{(2\epsilon + 1)R_0^3} \qquad (6)$$

where ϵ is the solvent dielectric constant, μ is the solute dipole moment, and R_0 is the radius of a sphere arbitrarily chosen to represent the first solvation shell. For illustration, we fix R_0 such that a sphere of radius R_0 has the same surface area as the solvent-accessible surface area[62] in the SM2 model for glucose. This yields 4.3 Å for R_0. Then eq 6 yields

$$\Delta G°_S = -0.09(\mu/D)^2 \text{ kcal/mol} \qquad (7)$$

for glucose in water, where $D = 1$ Debye. The dipole moments calculated for the various glucose rotamers range from 0.2 to 4.9 D, and eq 7 yields solvation free energies no more negative than about –2.1 kcal/mol for these dipoles. Thus it considerably underestimates the AM1-SM2 $\Delta G°_S$ values by about –18 to –19 kcal/mol. This represents a significant failure for this popular model which fails because it takes no account of several energetic effects associated with solvation (e.g., cavitation, dispersion, non-electrostatic components of hydrogen bonding, etc.).

The model does poorly even by comparison to ΔG_{ENP}, which includes only electrostatic and polarization effects. Thus, Figure 6 presents ΔG_{ENP} vs the square of the AM1 gas-phase dipole moment for the 33 rotamers in Table III as well as the remaining 5 from Table II. The solid line indicates the Onsager solvation free energy predicted from eq 7. For the majority of the rotamers, the polarization contribution to the solvation free energy is considerably greater than would be predicted from eq 7. Interestingly, for those rotamers with fairly large dipole moments, the trend is in the opposite direction. Indeed, the SM2 calculations predict that there is *no* correlation between ΔG_{ENP} and the square of the dipole moment; a linear regression of the data in Figure 6 affords a correlation coefficient R^2 that is less than 10^{-3}. We conclude that descriptions of molecular charge distribution that rely exclusively on the dipole moment are doomed to failure in molecules with multiple, internally polarized functional groups.

Further support for the large magnitude of the absolute free energies of solvation is provided by calculations using the AM1-

(59) Onsager, L. *J. Am. Chem. Soc.* **1936**, *58*, 1486.
(60) Reichardt, C. *Solvents and Solvent Effects in Organic Chemistry*, 2nd ed.; VCH: Weinheim, 1988.
(61) Wong, M. W.; Frisch, M. J.; Wiberg, K. *J. Am. Chem. Soc.* **1991**, *113*, 4776.
(62) (a) Lee, B.; Richards, F. M. *J. Mol. Biol.* **1971**, *55*, 379. (b) Hermann, R. B. *J. Phys. Chem.* **1972**, *76*, 2754.

SM1a[37,40] model. This model employs a different treatment of the dominant G°_{CDS} term, especially as regards the hydrogens, which it recognizes explicitly and treats in an environmentally sensitive fashion. The SM2 and SM3 models, on the other hand, give zero surface tension and surface area to the hydrogens themselves, but they adjust the heavy-atom surface tensions as a result of hydrogen attachment.[38-40] As a typical example of the calculated magnitude of the solvation free energy with the SM1a approach, the *tttt* rotamer is calculated to have a free energy of aqueous solvation of −17.1, −18.5, and −18.2 kcal/mol by the AM1-SM1a, AM1-SM2, and PM3-SM3 models, respectively.

The distributed monopole charge distributions used for the electric polarization effects in the SMx models permit a sensible explanation for the low calculated ΔG_{ENP} term for the *gg̃g̃g* rotamer. For *any* glucose rotamer characterized by a high degree of internal hydrogen bonding, there is an alternating series of negative (oxygen) and positive (hydrogen) atomic partial charges arrayed around the edge of the pyranose ring. Such a situation is poorly solvated by comparison to structures where unlike charge is sequestered into separated regions of space.[63] An inspection of Tables III and V indicates that, in general, as the total number of internal hydrogen bonds decreases, ΔG_{ENP} increases. So, for rotamers *g̃ggt*, *g̃g̃gt*, *g̃ggg̃*, and *g̃gtt*, which have the four largest AM1-SM2 ΔG_{ENP} terms, there are zero, one, zero, and one intramolecular hydrogen bonds, respectively. Conversely, rotamers *gg̃g̃g*, *g̃g̃g̃g*, and *tttt* are afforded some of the smallest ΔG_{ENP} values; each of them has the maximum possible (three) cyclic, internal hydrogen bonds.

Finally, we compare the structures found by optimization in aqueous solution to those optimized in the gas phase to provide an indication of the importance of solvent-induced geometric relaxation. In general, bond lengths and angles were only slightly affected by reoptimization of the geometry in the presence of solvent, with observed variations of about 0.002 Å and 0.4°, respectively. The interesting exception occurs for the anomeric O–C–O linkage, where aqueous solvation caused both C–O bonds to lengthen by up to 0.005 Å and the angle to widen by up to 1°. Torsional angles throughout the molecules, including those dictating rotation of the hydroxyl groups, typically changed by about 3°. Because of the dominance of the G°_{CDS} surface tension term in the free energies of solvation for all glucose rotamers, the effect of reoptimization in solution (which, given the relatively small impact on overall geometry, primarily affects the ΔG_{ENP} term) is not large. Nevertheless, geometric relaxation consistently accounted for an additional 0.1–0.2 kcal/mol of solvation free energy beyond that obtained from electronic relaxation alone.

All of the trends in solvation are reproduced with the PM3-SM3 model, as illustrated in part in Table VI and Figure 5. It is noteworthy that the two different models predict very similar absolute free energies of solvation for individual rotamers (Table V), although the ΔG_{ENP} term is slightly more important with the PM3-SM3 model. The enhanced polarizability of electronic structure using this model compared to AM1-SM2 has been noticed before; it is not as noticeable here as for extended π systems.[37]

Although the AM1-SM2 and PM3-SM3 models show close agreement for solvation free energies, the underlying AM1 and PM3 Hamiltonians provide drastically different pictures of the gas-phase rotameric hypersurface, as illustrated in Figure 4. The PM3 Hamiltonian considerably overstabilizes $-$ *-gg̃* rotamers by comparison to AM1 and ab initio[11] results. Evidently the favorable, antiparallel alignment of the dipoles of the C(3) and C(4) hydroxyl groups is more energetically stabilizing than are other arrangements which permit hydrogen bonding between these two groups.

This is particularly interesting in light of previous studies of the ability of semiempirical methods to model hydrogen bonding.[64] These studies compared AM1 and PM3 structures and energies for a variety of intermolecularly hydrogen bonded systems, and in general they found PM3 to be superior. In related work, Khalil *et al.*[65] also found that the AM1 model functions poorly in describing intermolecularly hydrogen bonded systems. However, they observed *excellent* performance for systems containing *intra*molecular hydrogen bonds, including β-fructopyranose. Indeed, the AM1 model outperformed a modified MNDO model[66] that was developed specifically for treating systems with *inter*molecular hydrogen bonds. The results presented here suggest that AM1 also performs better than PM3 for intramolecularly hydrogen bonded systems like carbohydrates. On the other hand, the AM1-SM2 and PM3-SM3 solvation models are in encouraging agreement with each other for solvation free energies for given glucose rotamers, indicating that predictions of this quantity may be more reliable than gas-phase solute energies.

5. Concluding Remarks

The present quantum chemical calculations show little difference in the free energies of aqueous solvation for the α and β anomers of glucose, in contrast to previous explicit water simulations based on molecular mechanics. Our calculations indicate that the net effect of solvation makes no contribution to the free energy of mutarotation. Unfavorable solvation of the *T* conformation of the hydroxymethyl group, on the other hand, does appear to play a sizable role in destabilizing it relative to the $\bar{G}$ and *G* conformations, which are the only two observed experimentally.[13]

On the basis of the AM1-SM2 results, it appears that at least two other conformations resulting from rotation of the non-anomeric, ring hydroxyl groups are significantly populated at equilibrium. Additionally, exo-anomeric orientations of the C(1) hydroxyl group are not significantly stabilized over the *anti* (*t*) conformation when the latter orientation allows participation in a prearranged, clockwise array of intramolecular hydrogen bonding. In general, such arrays of conjugated hydrogen bonds are somewhat less well solvated than rotamers with disrupted hydrogen bonded patterns, but they are still stable enough to be well populated in solution.

For the ring hydroxyl rotameric equilibria, we find that electric polarization effects rather than specific hydrogen bonding effects provide the dominant differential solvation effects, but the popular assumption that dielectric polarization correlates with the overall dipole moment is not born out, even qualitatively.

Acknowledgment. This work was supported in part by supercomputer resources made available by the University of Minnesota Supercomputer Institute and by funding from the National Science Foundation and the Army ILIR Program.

(63) Cramer, C. J.; Truhlar, D. G. *J. Am. Chem. Soc.* **1992**, *114*, 8794.

(64) Zheng, Y.-J.; Merz, K. M., Jr. *J. Comput. Chem.* **1992**, *13*, 1151.

(65) Khalil, M.; Woods, R. J.; Weaver, D. F.; Smith, V. H., Jr. *J. Comput. Chem.* **1991**, *12*, 584.

(66) Voityuk, A. A.; Bliznyuk, A. A. *Theor. Chim. Acta* **1987**, *72*, 223.